

Theory of Insulator Metal Transition and Colossal Magnetoresistance in Doped Manganites

T. V. Ramakrishnan[*], H. R. Krishnamurthy[*], S. R. Hassan[*] and G. V. Pai[†]

Centre for Condensed Matter Theory, Department of Physics,
Indian Institute of Science, Bangalore 560 012, India

(dated: March 22, 2024)

The persistent proximity of insulating and metallic phases, a puzzling characteristic of manganites, is argued to arise from the self organization of the twofold degenerate e_g orbitals of Mn into localized Jahn-Teller (JT) polaronic levels and broad band states due to the large electron-JT phonon coupling present in them. We describe a new two band model with strong correlations and a dynamical mean-field theory calculation of equilibrium and transport properties. These explain the insulator metal transition and colossal magnetoresistance quantitatively, as well as other consequences of two state coexistence.

PACS numbers: 75.47.Lx, 75.47.Gk, 71.27.+a, 71.30.+h, 71.38.-k

Doped perovskite manganites $\text{Re}_{1-x}\text{A}_x\text{MnO}_3$, where Re and A are rare earth and alkaline earth ions, show a rich variety of electronic, magnetic and structural phenomena and phases [1, 2]. Unusual effects, such as insulator-metal (IM) transitions both as a function of x and of temperature T over a wide region $x < 0.5$, or even as a consequence of isotope substitution ($^{18}\text{O} \rightarrow ^{16}\text{O}$) [3], colossal magnetoresistance (CMR) near T_{IM} and ‘melting’ of the charge/orbitally ordered insulator ($x > 0.5$) into a metal in a relatively small (5-7 Tesla) magnetic field all suggest that metallic and insulating phases are always very close in free energy. This is also reflected in the ubiquitous coexistence (static or dynamic) of two ‘phases’, one insulating with local lattice distortion and the other metallic without lattice distortion, with length scales varying from 10 Å to 10^3 Å [2].

These phenomena are due to the dynamics of the e_g electrons of Mn constrained by three strong on-site interactions, namely electron lattice or Jahn-Teller (JT) coupling which splits the twofold e_g orbital degeneracy, ferromagnetic e_g spin- t_{2g} spin exchange or Hund’s coupling J_H and e_g electron repulsion U . The respective energies are $E_{\text{JT}} \sim 0.5$ eV, $J_H \sim 2$ eV and $U \sim 5$ eV, compared to the e_g electron intersite hopping $t \sim 0.2$ eV which sets the kinetic energy scale [4]. Understanding their observed consequences is one of the major challenges in the physics of strongly interacting electrons. Earlier theoretical attempts neglect one or more of these strong interactions and make further approximations; the predictions do not agree with many characteristics of manganites. For example the ferromagnetic Curie transition in a number of manganites is from an insulator to a metal, for $0.2 < x < 0.5$. However, a theory with just Hund’s coupling, due to Furukawa [5], finds only a metallic phase, while Millis, Muller and Shraiman [6], who additionally include the electron-JT phonon coupling g but treat the JT distortions as static displacements, obtain a metal-metal transition crossing over to an insulator-insulator

transition as g increases.

We propose and implement here a new approach which incorporates the crucial effects of all the three interactions and is based on a new idea, namely that of coexisting JT polaronic and broad band e_g states, which we believe is the key to manganite physics. The idea and some of its consequences are described and calculations based on a new two band model are then outlined.

We first discuss the effect of large JT coupling g on the initially twofold degenerate e_g orbitals at each lattice site. There is one superposition (labelled ‘a’) which, when singly occupied, leads to a polaronic state with local octahedral symmetry breaking Mn-O bond distortion and energy E_{JT} . Its intersite hopping is reduced (for $E_{\text{JT}} = \hbar \omega_0$) to t_0 where ω_0 is the JT phonon mode frequency) by the exponential Huang-Rhys [7] or phonon overlap factor $\exp(-E_{\text{JT}}/2\hbar\omega_0)$. Since $\omega_0 \sim \exp(-5)$ for LaMnO_3 , and being a local quantity is not likely to change much on doping, the ‘polaron bandwidth $2D = 2zt_0 \sim k_B(125\text{K})$ is small, and is neglected in much of this paper. At each site, there is necessarily another, orthogonal state (labelled ‘b’). Its energy is zero on the fraction x of sites where the ‘a’ electrons are not present (hole-sites), and is $U = (U + 2E_{\text{JT}})$ on the ‘b’ electron sites. The ‘b’ electron hops adiabatically with $t_0 \sim \omega_0^{-1}$, in an annealed random medium of repulsive ‘sites and (for a homogeneous orbital liquid) form a band whose renormalized bandwidth $2D$ increases with x as well as with T^{-1} and H . For, the inhibition of hopping due to large U is reduced when there are more hole-sites, and that due to large J_H is reduced when the t_{2g} spin order is enhanced. We show in this paper that the simultaneous presence of ‘polaron states and the ‘b’ band, the change in the effective bandwidth of the latter with $x; T; H$ etc. and the consequent change in their relative occupation (leading to an insulator eg for $E_{\text{JT}} > D$ and metal for $E_{\text{JT}} < D$) are the basis of many phenomena seen in manganites. Our picture requires the persistence of local JT distortions well into the metallic regime, as

indeed seen by direct probes of instantaneous Mn-O bond length [8]. The σ polaron motion is anti-adiabatic ($2D \ll \hbar!_0$) while the b electron motion is adiabatic ($2D \gg \hbar!_0$); the respective bandwidths are exponentially small and of order the bare value. By contrast, in earlier theoretical work [6, 9] where the JT distortion is treated as static, both σ and b electron dynamics become adiabatic so that the bands are of comparable width, leading to consequences which disagree with experiment.

The system of correlated σ and b states described above can be modelled by the Hamiltonian

$$H_b = \left(E_{JT} \right) \sum_i \psi_i^\dagger \psi_i + \sum_i b_i^\dagger b_i + t \sum_{\langle ij \rangle} (b_i^\dagger b_j + \text{hc}) + U \sum_i n_{\sigma i} n_{bi} + H_m \quad (1)$$

In Eq.(1), the σ polaron has energy (E_{JT}), the b electrons hop between nearest neighbour sites with an effective amplitude t , and U is the effective repulsion between σ polarons and b electrons of the same spin at a particular site [10]. The common chemical potential is μ . H_m is the magnetic part involving the e_g spins S_i and t_{2g} core spins S_i , namely

$$H_m = J_H \sum_i S_i \cdot S_i + J_F \sum_{\langle ij \rangle} S_i \cdot S_j + \sum_i S_i \cdot H \quad (2)$$

In addition to the familiar Hund's coupling J_H and Zeeman coupling to an external field H (neglecting the relatively smaller term $\sum_i S_i \cdot H$) we have included in H_m a new ferromagnetic nearest neighbour exchange J_F between the t_{2g} core spins.

The new term arises from a virtual double-exchange process in which an σ electron at a site i hops quickly (adiabatically) to a nearest neighbour site j and back. In the limit of large U and J_H , and approximating the t_{2g} spins as classical, i.e., $S_i = \hat{S}_i$ where \hat{S}_i are unit vectors, the energy shift to second order in t is $t^2 = 2E_{JT} \frac{1}{2} (\hat{S}_i \cdot \hat{S}_j + 1) (n_{\sigma i}(1 - n_{\sigma j}) + n_{\sigma j}(1 - n_{\sigma i}))$. The energy denominator $2E_{JT}$ arises from the unrelaxed JT distorted intermediate state, the $\frac{1}{2} (\hat{S}_i \cdot \hat{S}_j + 1)$ factor from large J_H , and the occupancy dependent terms from large U . We have further approximated this by the simple exchange term in Eq.(2), whence $J_F = t^2 = (2E_{JT} S^2) x(1 - x)$.

The model Hamiltonian H_b (Eq.(1)) can be motivated starting from a lattice model with two e_g orbitals per site [1, 2]. Let a_i^\dagger create an electron in orbital at site i , (with $j = 1 > j^2 > y^2 >$ and $j = 2 > j^2 > z^2 >$ say), locally coupled to JT lattice modes ($Q_{xi}; Q_{zi}$) ($Q_i; i$) by the term $H_{JT} = g a_i^\dagger \sim a_i Q_i$ where \sim are the Pauli matrices. The eigenvalues of H_{JT} are $\pm gQ_i$, the corresponding electron creation operators being labelled b_i^\dagger and ψ_i . The effective lattice potential energies for single electron occupation of these states are

$(K=2)Q_i^2 - gQ_i$ where K is the phonon force constant. The lower (ψ) branch has a minimum at a static lattice distortion $Q_0 = g/K$ and energy $E_{JT} = (g^2/2K)$. ψ_i in Eq.(1) are polaron creation operators given by $\psi_i = \hat{U}_i \psi_i$ where $\hat{U}_i = \exp(iQ_0 P_i / \hbar)$ where P_i is the radial momentum conjugate to Q_i) are unitary Lang-Firsov [11] like displacement transformations. The exponential reduction in the hopping amplitude of ψ arises essentially from their ground state average. (We neglect the small fluctuations with respect to this average). No lattice distortion or reduction in hopping is associated with the higher (b) branch. The small leading intersite term $H_b^0 = t \sum_{\langle ij \rangle} \psi_i^\dagger b_j + b_i^\dagger \psi_j + \text{hc}$ describing ψ - b hybridization is not included in Eq.(1); some consequences are discussed later. Thus for ($E_{JT} = \hbar!_0$) ~ 1 , and neglecting H_b^0 , we are led to Eq.(1). We have made further approximations which are realistic for a homogenous orbital liquid, by statistically averaging quantities which depend on the orbital admixture angle f_{ig} , eg the intersite hopping and the nearest neighbour Mn-O bond correlations (short-long), so that t and b_i^\dagger are to be regarded as averaged over f_{ig} . This is reasonable for $0.2 < x < 0.5$ in most manganites, but poor for those other values of x for which one has strong orbital correlations or long range orbital order. Finally, in this regime, the chemical potential is chosen such that

$$n_{\sigma i} + n_{bi} = n_{\sigma} + n_b = (1 - x) \quad (3)$$

We have calculated the equilibrium and transport properties of H_b (Eq.(1)) using the dynamical mean field theory (DMFT) [12] which is exact in $d=1$, and is accurate in three dimensions if spatial correlations are not crucial. H_b , being a generalized form of the Falicov-Kimball model [13] with additional spin interactions H_m (Eq.(2)) and constraint Eq.(3), is exactly soluble in this limit [12]. We treat the t_{2g} core spins as classical as stated earlier, and their interaction in the Curie-Weiss mean field approximation, and work in the large J_H limit (i.e. $S J_H = t \sim 1$). The local self-energy $\Sigma_i(!^+)$ of the b electrons and the mean magnetization $m = \langle \hat{S}_i \rangle$ are determined self-consistently. From these we calculate the spectral density or density of states (DOS) $\rho_b(!)$ of the b electrons which determines their occupation relative to that of the ψ state, the current-current correlation function relevant for the Kubo formula for the electrical conductivity, etc [14]. Most of our calculations use a semicircular bare DOS with a bare bandwidth $2D_0$ [15].

Our results for $\rho_b(!)$ for different values of x and T are shown in Fig.1. Since the effective bandwidth $2D$ of the b electrons decreases significantly as x decreases (for any sizeable U), the b band bottom is above the ψ level for small x e.g. $x = 0.1$ (Fig.1a), and the low temperature state is an insulator, ferromagnetic because of J_F . (We ignore the anti-ferromagnetic super-exchange as it is dominated by the much larger J_F for $x > 0.1$). On

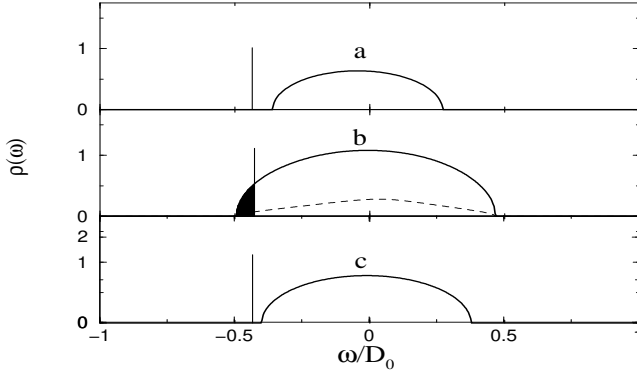


FIG. 1: Spectral density or b-DOS $\rho(\omega)$ for various values of doping x and temperature T . The effective 'polaron level' is marked as a vertical line. Parameters chosen are $E_{JT} = 0.5 \text{ eV}$, $D_0 = 1.2 \text{ eV}$, $U = 5.0 \text{ eV}$, $J_F = 2.23 \text{ meV}$. (a) $x = 0.1$, $T = 0$, $\mu = E_{JT}$; ferromagnetic insulator. (b) $x = 0.3$, $T = 180 \text{ K}$ ($< T_c = 240 \text{ K}$); ferromagnetic metal. (c) $x = 0.3$, $T = 350 \text{ K}$; paramagnetic insulator. Full (dotted) lines correspond to up (down) spin DOS. Occupied band states are shown shaded.

increasing x , D increases as well, and beyond a critical x_c for which $D = E_{JT}$, the low temperature state is a ferromagnetic metal, as in Fig.1b. We note that while both b and \backslash states are occupied in the metal, most electrons are in the latter, polaronic state since $n_{\backslash} = 0.66$ and $n_b = 0.04$. T_c is largely due to J_F ; for n_b being very small, so is the b electron contribution to T_c via conventional double exchange. On increasing T at this x , the t_{2g} spins disorder, reducing the effective b electron hopping or D . Fig.1c shows the DOS at $T = 350 \text{ K}$ ($> T_c$). It is that of a small gap semiconductor. The metal-insulator transition occurs very near T_c because of the strong feedback between D and the magnetization m . The carriers in the paramagnetic state are b electrons excited across the relatively small effective band gap, not thermally unbound small polarons. The mobile carrier fraction n_b is very small in the metallic phase ($n_b \sim 0.06$ for parameters corresponding to $\text{La}_{0.7}\text{Sr}_{0.3}\text{MnO}_3$) and decreases rapidly [14] to a minimum at T_c , whereas the electron density is 0.7 per site. This is exactly the hitherto unexplained inference for n_{eff} from the observed D nude weight in this compound [16].

Our theory also describes transport properties fairly well. Fig.2 shows the electrical resistivity $\rho(T)$ versus T for model parameters chosen to fit T_c and (T_c) for $\text{La}_{0.67}\text{Ca}_{0.33}\text{MnO}_3$ [17]. The results for semicircular DOS and tight binding DOS are nearly the same. We see clearly the sharp paramagnetic insulator to ferromagnetic metal transition, the former having a calculated effective electrical gap ρ_{eff} of 34 meV while the experimental value is 48 meV [18]. The resistivity falls dramatically to about $2 \text{ m}\Omega\text{cm}$ just below T_c and does not decrease much further thereafter, in contrast to the observed residual re-

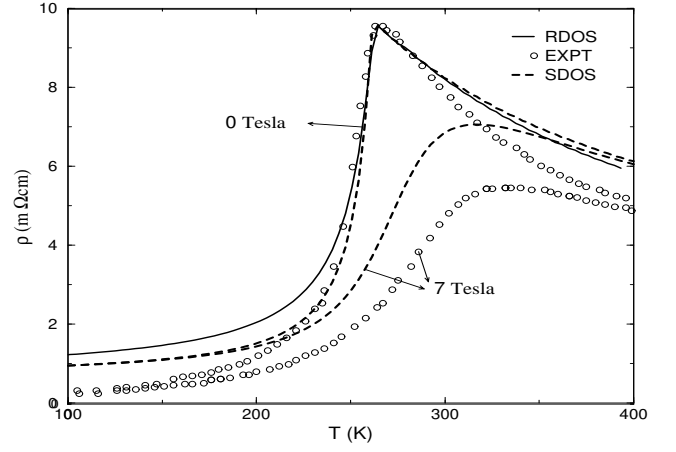


FIG. 2: The resistivity $\rho(T)$ of $\text{La}_{1-x}\text{Ca}_x\text{MnO}_3$ ($x = 0.33$) as a function of temperature T . Calculated (full lines for realistic anisotropic hopping, dotted lines for a semicircular DOS) and experimental (circles, from ref.[17]) results for $H = 0$ and 7 Tesla are shown. Parameters, chosen to fit T_c and (T_c) , are $E_{JT} = 0.5 \text{ eV}$ (SDOS), 0.6 eV (RDOS), $2D_0 = 2.4 \text{ eV}$ (SDOS), 2.44 eV (RDOS), $U = 5 \text{ eV}$, and $J_F = 2.37 \text{ meV}$.

sistivity values which can be as small as $50 \text{ m}\Omega\text{cm}$. This is a consequence of our neglect of inter-site 'coherence and is discussed later. The resistivity in a field of 7 Tesla is also shown in Fig.2. The colossal decrease (CMR) is apparent [18].

The properties of manganites vary strongly and characteristically with the ionic species Re and A . This is natural in our model, since the relative balance between metal and insulator is strongly affected by small changes in E_{JT} and D_0 and the carrier density depends exponentially on $(D - E_{JT})$. For example, keeping E_{JT} fixed (for a given $x = 0.3$ say), and varying $2D_0$, we find the variations in physical properties shown in Fig.3. T_c , being proportional to J_F , increases roughly as D_0^2 . The Curie transition changes from insulator-insulator to insulator-metal to metal-metal, as is seen experimentally in the sequence $\text{Pr}_{0.7}\text{Ca}_{0.3}\text{MnO}_3$; $\text{La}_{0.7}\text{Ca}_{0.3}\text{MnO}_3$ and $\text{La}_{0.7}\text{Sr}_{0.3}\text{MnO}_3$. D_0 is believed [19] to increase in this order. We also exhibit the enormous variation in the calculated fractional magneto-resistance $f_R(H) = \rho(H)/\rho(T=T_c)$ for $H = 7 \text{ Tesla}$ as a function of T_c ; the agreement with experiment [20] is very good.

Thus, in the regime $0.2 < x < 0.4$, a wide range of physical properties for a number of doped manganites can be understood physically and described quantitatively by our theory [14]. The ratio (E_{JT}/D_0) broadly determines the systematics and D_0 the basic energy scale (J_H and U being close to 1 for our purposes).

The intersite hopping of the \backslash polarons arising from term H_{\backslash}^0 , with a characteristic temperature scale of $T_{\backslash} = (z t = k_B)^{-1} \sim 125 \text{ K}$, has many important consequences. Below T_{\backslash} the \backslash states can form a coherent band

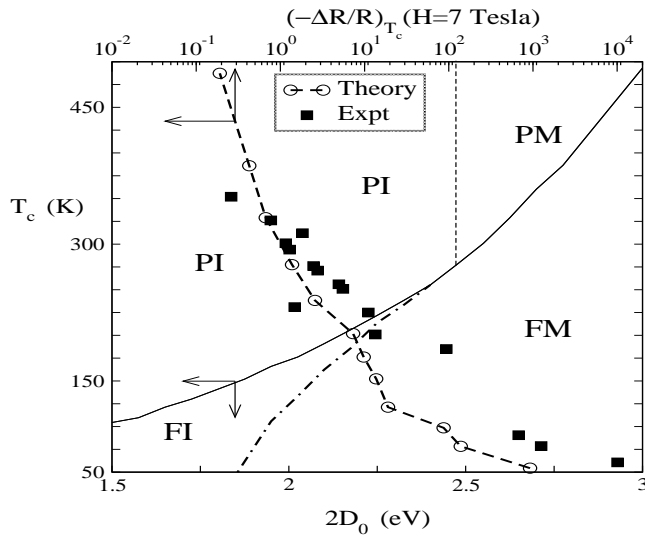


FIG. 3: Physical properties as a function of the d electron bandwidth $2D_0$, for fixed $E_{JT} = 0.5$ eV. Full line: ferromagnetic T_c vs D_0 . The resistive transition is from an insulator to a metal (PI-FI) for small D_0 , from an insulator to a metal (PI-FM) for intermediate D_0 , and from a metal to a metal (PM-FM) for large D_0 , as indicated. Broken line: calculated fractional magnetoresistance $(-ΔR/R)_{T_c}$ vs T_c for $H = 7$ Tesla. Experimental points are from [20].

due to hybridization with b states, whence the JT distortion can become dynamic (time scale $\hbar/k_B T$), and also smaller self-consistently. The b electron scattering and the consequent resistivity then vanish at $T = 0$, and are nonzero only if static disorder is present. This can lead to a metallic state with a small residual resistivity or to an Anderson localized insulating state depending on the amount of disorder. The strong dependence of T_c on isotope mass M_0 is also a consequence of 'polaron hopping, since its direct double exchange contribution to T_c will be proportional to $t(1-x)\exp(-E_{JT}/2\hbar\omega_0)$ and $\omega_0 = \hbar/KM_0$. The isotope effect thus estimated is of the right size [21].

Spatial correlations and inhomogeneities can be investigated in an extended version of the model in Eq.(1) by including the orbital angles ϕ_i as additional degrees of freedom. The intersite hopping t_{ij} now depends on ϕ_i and ϕ_j . There are a number of anharmonic, steric, elastic terms, eg., nearest neighbour long-short Mn-O bond correlations, coupling between JT modes and strain, etc., which depend on these angles as well. These, and other factors such as the variation of E_{JT} with local ion size, can be included in Eq.(1), and questions such as short range correlation, orbital order, long range order in $(n_i - n_{bi})$ (total charge/relative charge order), disorder induced 'phase' separation, explored by going beyond the self-consistent single site DMFT used here. It would also be interesting to explore the idea of exponentially separated time scales and adiabatic-nonadiabatic crossover

in other oxides and organic molecules with orbital degeneracy and strong local symmetry breaking Jahn Teller coupling.

We would like to acknowledge support from the Indo-French Centre for Promoting Advanced Research grant 2404-1 (HRK), US-India project ONR N 00014-97-0988 (TVR) and the Council for Scientific and Industrial Research, India (SRH, GVP).

[*] Also Condensed Matter Theory Unit, JNCASR, Jakkur, Bangalore 560 064, India.

[y] Also Abdus Salam International Centre for Theoretical Physics, 11 Strada Costiera, Trieste 34014, Italy

[1] For reviews, see Colossal Magnetoresistance Oxides, ed Y Tokura (Gordon and Breach, New York, 2000); M B Salamon and M Jaime, Rev. Mod. Phys. 73, 583 (2001).

[2] eg. Nanoscale Phase Separation in Manganites by E Dagotto (Springer Verlag, New York and Heidelberg, 2002).

[3] N A Babushkina, et al., Nature 391, 159 (1998).

[4] see eg. D D Sarma et al., Phys. Rev. Lett. 75, 1126 (1995), S Satpathy, Z S Popovic, and F R Vukajlovic, Phys. Rev. Lett. 76, 960 (1996).

[5] N Furukawa, Journal of the Physical Society of Japan, 64 2734 (1995).

[6] A J Millis, R Mueller and B I Shraiman, Phys. Rev. B 54, 5389, 5405 (1995).

[7] K Huang and F Rhys, Proc. Roy. Soc. London Ser. A 204, 406 (1950).

[8] see for example the pulsed neutron measurements of D. Louca et al., Phys. Rev. B. 56, R8475 (1997). and the EXAFS results of C Meneghini et al., J Phys. Cond. Matt. 14, 1967 (2002).

[9] M S Laad, L Craco and E Muller-Hartmann Phys. Rev. B 63, 214419 (2001).

[10] We neglect same site opposite spin interactions since such configurations are strongly disfavoured in the large J_H limit we treat in this paper.

[11] G I Lang and A Yu Firsov, Soviet Physics JETP 43, 1843 (1962).

[12] A Georges, G Kotliar, W Krauth and M J Rozenberg, Rev. Mod. Phys. 68, 13 (1996).

[13] L.M. Falicov and J C Kimball, Phys. Rev. Lett. 22, 997 (1969).

[14] Details as well as additional new results will be published elsewhere.

[15] We find that the calculated results are nearly the same for semicircular DOS and realistic tight binding DOS (eg. see Fig.2 for resistivity).

[16] Y. Okimoto, et al., Phys. Rev. B 55, 4206 (1997).

[17] G. J. Snyder et al., Phys. Rev. B 53, 14434 (1996).

[18] The discrepancies can be reduced within our model by including short-range correlations which are neglected in the DMFT.

[19] H. Y. Hwang et. al., Phys. Rev. Lett. 75, 914 (1995).

[20] K Khazen et al., Phys. Rev. Lett. 76, 295 (1996).

[21] G. M. Zhao, et al., Phys. Rev. B 63, 060402 (2001).